ELSEVIER

Journal of Nuclear Materials 257 (1998) 274–281

journal of nuclear materials

Comparison of hot dip aluminised F82H-mod. steel after different subsequent heat treatments

H. Glasbrenner *, O. Wedemeyer

Forschungszentrum Karlsruhe GmbH, Institut für Materialforschung III, P.O. Box 3640, D-76021 Karlsruhe, Germany

Received 10 February 1998; accepted 10 June 1998

Abstract

A homogeneous intermetallic phase with a thickness of about 20–30 μm was formed on the surface of the steel F82H-mod. during hot dip aluminising at 700°C for 30 s. The transformation behaviour of this compound Fe_2Al_5 was investigated by two different heat treatment procedures: the standard heat treatment for F82H-mod. steel (1040°C/0.5 h, 750°C/1 h) and for MANET steel 1075°C/0.5 h, 750°C/2 h). The structure of the transformed coating shows an internal and an external layer separated by a porous band independent of the heat treatment. The internal layer consists of α-Fe(Al), the external of FeAl. On top of the coating a thin alumina layer is observed. The thickness of the internal layer and the phase of the formed alumina layer are influenced by the chosen heat treatment.

1. Introduction

One of the main issues in the design of blankets for a future fusion reactor is the permeation of tritium through the structural material into the secondary circuit [1–3]. In the case of the water-cooled liquid Pb–17Li blanket the concentration of tritium in the cooling water has to be minimised for safety and economical reasons. A martensitic steel at present foreseen as structural material cannot be used without any further protection to reduce the tritium permeation. One of the most promising methods entails the use of coatings which have low diffusion rates and/or low hydrogen recombination and adsorption constants.

It is well known that thin alumina layers can reduce the tritium permeation rate by several orders of magnitude [4–6]. Hence, the development of alumina layers as a TPB (tritium permeation barrier) on a martensitic steel is the main effort. The requirements raised up to the permeation barrier fabrication technique are the following:

- formation of a permeation barrier on a structural material in the required metallurgical state at the end of the fabrication process;
- supply of a coating with acceptable properties, e.g. a tritium permeation reduction factor PRF $\geqslant$ 100 under reactor conditions;
- compatibility with the ITER test module geometry and fabrication sequence.

In this paper the complete characterisation of aluminised coatings by means of the hot dip procedure on the structural material F82H-mod. will be presented. The effect of two different heat treatments – the two standard heat treatments of the martensitic steels F82H-mod. and MANET – on aluminised samples will be discussed.

2. Preparation of the coating

2.1. Materials

The substrate material to be aluminised was the fully martensitic steel F82H-mod. The material was produced by JAERI/NKK Corporation, Japan with the following nominal composition (wt%); C, 0.09; Mn, 0.156; Cr,

* Corresponding author. Tel.: +49-7247 823 723; fax: +49-7247 823 956; e-mail: glasbrenner@imf.fzk.de.

0022-3115/98/$ – see front matter
PII: S0022-3115(98)00456-5

8.36; Ni, 0.021; Mo < 0.0003; V, 0.162; Nb, 0.01 and the balance being Fe. Al used for the melt has an initial purity of 99.5% with the main impurities being Fe and Si. The melt became enriched in the main steel components Fe and Cr with increasing immersion time.

2.2. Sample preparation

The material was delivered as 20 mm thick sheets (F82H-mod.) in a tempered condition. Sheet specimens of $50 \times 15 \times 1$ mm^3 were machined by erosion. Each sample had a small hole on one side for fixing during the aluminising process. After machining the samples were degreased in acetone and finally cleaned ultrasonically in ethanol. As a final surface preparation the cleaned specimens were dipped into a flux solution (solution of KCl, NaCl and Na_3AlF_6 (mass ratio 5:4:1) in water) and dried.

2.3. Aluminising process

Aluminising has been carried out by using a special facility developed in FZK [7]. A heated alumina crucible is connected gas-tight to the bottom of a glove box. A reducing Ar–5%H_2 gas mixture was used as working atmosphere since oxidation of the Al melt had to be avoided. The alumina crucible was filled with small Al pieces and heated up to 700°C. The temperature was measured by a NiCr–Ni thermocouple which was protected by an alumina tube and placed directly in the Al melt. The samples were fixed by a hook and a stainless steel wire to a crane system and were dipped into the melt. They were pulled out of the melt after 30 s of exposure. Cooling down took place in the glove box by natural cooling rate.

2.4. Heat treatment

In order to optimise the coating structure in view of the demands of a tritium permeation barrier a suitable heat treatment has to be carried out after aluminising. The goal of a successful heat treatment process should include:

- complete incorporation of solidified aluminium on the sample surface into the steel matrix by diffusion;
- transformation of the brittle intermetallic Fe_2Al_5 layer which formed during the aluminising process, into more ductile phases (preferable FeAl and/or α-Fe(Al)) by diffusion of aluminium into the steel matrix;
- formation of a thin alumina layer on top of the coating as a very efficient tritium permeation barrier with the potential for self-healing;
- the formed alumina layer has to be compatible with Pb–17Li or water under the particular conditions required which is dependent of the location of the coating (inside or outside of the tubes);
- the preparation process of the coating has to be compatible with the heat treatments admissible for the steel to guarantee the original mechanical properties of the structural material under working conditions after coating;
- the whole coating system should be kept as thin as possible since aluminium is an activating element and is not desired in the matrix of low activation steels.

The heat treatment was carried out in a horizontal quartz rig. The aluminised samples were cleaned ultrasonically in ethanol, dried and placed in alumina crucibles which were positioned in the hot zone of the furnace. The working rig was flushed with argon (impurities $\leqslant 10^{-4}$%) and finally a flow rate of 5 l/h and a pressure of 1.25 bar were set. The heating rate was about 25 K/min. After the required holding time the crucibles were removed from the hot zone of the furnace and cooled down in air. Time and temperature regimes of the chosen heat treatments are listed in Table 1.

Extended investigations have shown that the fulfillment of the demands listed above requires reaustenitisation and subsequent tempering of the aluminised samples. Type A is the standard heat treatment of steel F82H-mod. Type B heat treatment corresponds to the standard heat treatment for MANET steel. Additionally, an aluminised F82H-mod. sheet was austenised and tempered under MANET conditions (Type B) for better comparison with the results obtained previously [8,9].

Table 1
Time and temperature regimes of the heat treatments after aluminising

Type/material	Aluminising conditions	Heat treatment
A/F82H-mod.	700°C/30 s	1040°C/0.5 h/air cooling 750°C/1 h/air cooling
B/F82H-mod.	700°C/30 s	1075°C/0.5 h/air cooling 750°C/2 h/air cooling

3. Basic characterisation of the coating

3.1. Aluminised samples

3.1.1. Metallographic examination

After aluminising the samples were homogeneously covered by an overlayer of the solidified Al melt. The thickness of this layer varies strongly. A drop of Al solidified on the bottom side of each sample during the cooling phase since no tools were used to remove the melt drop. An intermetallic layer formed mainly beneath the Al overlayer at about 20–30 μm thick by Al diffusion into the steel substrate. The interface between the substrate and the intermetallic layer is smooth although the layer grew somewhat tongue-like into the substrate. The interface between the Al overlayer and the intermetallic layer appears very inhomogeneous. This pattern is a good indication for two alternative processes: Crystal growth and dissolution of the crystals formed and were transported into the Al melt. Some cracks could be observed across the intermetallic layer.

3.1.2. Analytical examination

SEM/EDX point analyses of hot dip aluminised samples have shown that the main part of the layer corresponds to the Fe_2Al_5 phase. The interface of the intermetallic layer shows just beneath the solidified Al a higher Al concentration compared to the rest of the layer indicating the existence of the $FeAl_3$ phase. The striation like precipitates in the Al melt were found to be $FeAl_3$ phase as well.

EPMA line scans of an aluminised F82H-mod. sheet are given in Fig. 1. The Al content decreases continuously from nearly 100 at.% down to around 71 at.% in the first few microns. The values of the measured iron content show the opposite trend: from 0 at.% at the near surface region up to around 28 at.% in the depth of 5 μm. The concentration of all elements measured are rather constant in a depth range of about 5–25 μm. This composition conforms to Fe_2Al_5 phase as well. On the transition zone from Fe_2Al_5 phase to the steel matrix, the concentration of the elements rapidly changes.

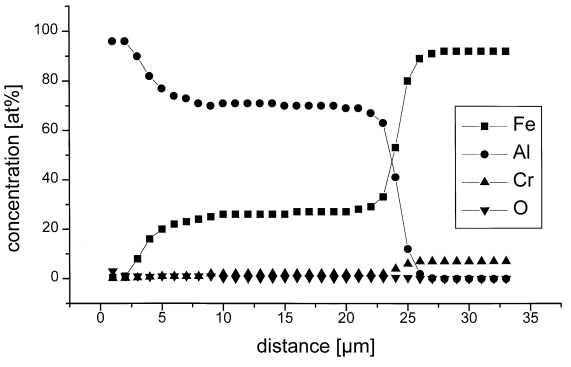

Fig. 1. EPMA line scans carried out on the cross section of an aluminised F82H-mod. sheet.

3.1.3. Vickers microhardness

The microhardness of the formed intermetallic layer after the aluminising process was about 800–1100 HV 0.05, independent of the composition of the structural material. This is in good agreement with microhardness values for the compound Fe_2Al_5 reported in the literature (1125 HV 0.05 [10], 835 HV 0.2 [11]). The microhardness of the substrate remained unchanged compared to the virgin material.

3.2. Aluminised and subsequent heat-treated samples

3.2.1. Surface investigation

In the XPS spectra of type A and B samples the elements Al and O can be clearly detected. No photopeaks of the steel elements Fe or Cr were detected in the spectra. The detection limit for this method is 0.1–1.0 wt%. In Fig. 2 the Al 2p photopeaks of each sample investigated are shown. An increase of the binding energy of the Al 2p peak from 72.9 eV (type A) to 73.3 eV (type B) can be observed. Additionally, the FWHM decreases from around 2.5 eV down to 2.2 eV. The conclusion of these observations can be summarised as follows: The surface exists of pure alumina. The heat treatment of type A samples leads to different alumina compounds but is not sufficient to form α-Al_2O_3. In contrast to these results type B heat-treated samples exist mainly of α-Al_2O_3 on the surface [12].

The aluminised and subsequently heat-treated F82H-mod. samples were analysed with low angle XRD in order to get information on the compounds existing on the surface. The diffractogram for type A sample is given in Fig. 3. The main reflex comes either from FeAl or Fe_3Al phases or from both. These two compounds cannot be exactly identified by this method. The spectrum for type B samples is given as well in Fig. 3. In comparison with the type A diffractogram more additional reflexes can be observed for type B. These peaks can be clearly related to α-Al_2O_3. For better comparison the signals for this compound were added to the diffractogram as lines. It can be easily seen that α-Al_2O_3 is formed at 1075°C within 30 min., but not at 1040°C. It is known that α-Al_2O_3 is also formed at 1040°C but unfortunately at this temperature the transformation requires longer times. This result is in agreement with the XPS measurements discussed above.

EDX measurements with working voltages from 10 to 30 keV were carried out on type A and B samples. The measurements on both samples show the same results. The high Al content measured in the near surface (up to a thickness of ~0.7 μm) indicates that an

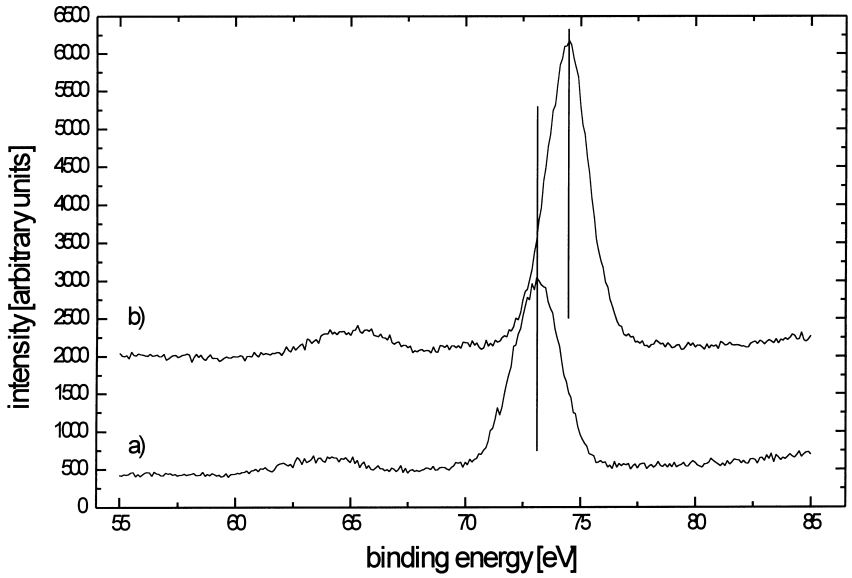

Fig. 2. Al 2p photopeak of (a) type A heat treated sample (1040°C, 30 s and 750°C, 1 h) and (b) type B heat treated sample (1075°C, 30 s and 750°C, 2 h).

oxidation process has occurred which is in agreement with the results obtained with XPS and low angle XRD. Beneath this enriched Al layer, the Al content is found to be reduced.

In contrast to the EDX results, SEM investigations have shown that the morphology of the sample surfaces appears different for type A (1040°C/0.5 h, 750°C/ 1h) and B (1075°C/0.5 h, 750°C/2 h). The surface structure

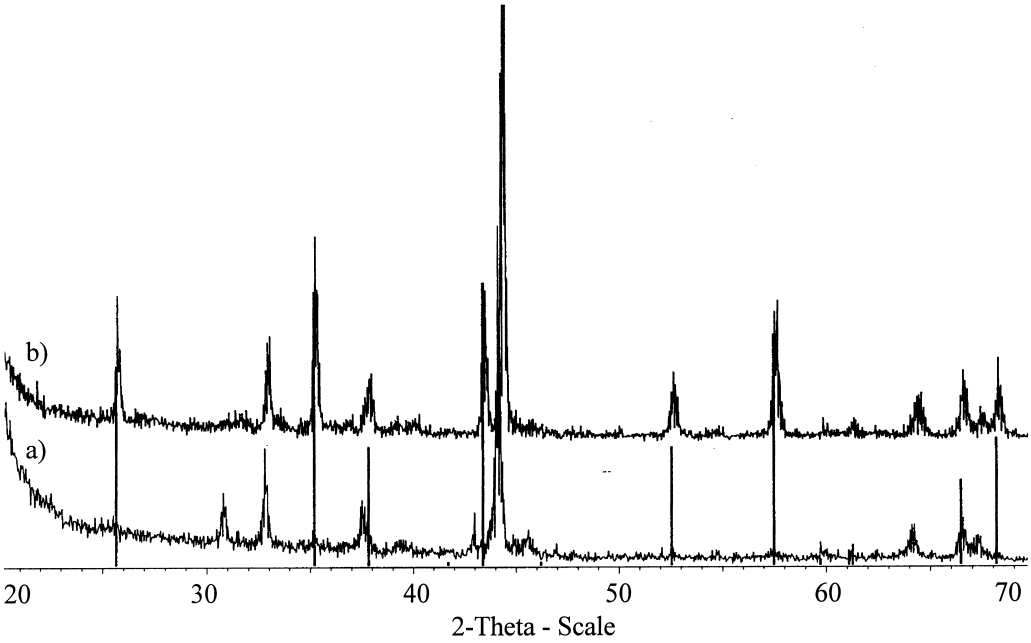

Fig. 3. Low angle XRD diffractogram of aluminised F82H-mod. (a) type A and (b) type B samples. The signals for α-Al_2O_3 were added to the spectra as lines.

of type A samples is fine-grained and homogenous at any point on the samples. No cracks or voids and even no corrosion products can be observed all over the samples.

The surface morphology of type B samples is more structured than the surface obtained for type A. The layer covers the whole surface homogeneously with a pronounced texture. Additionally, some cracks revealed in the surface layer and corrosion products with a size up to about 50 μm were formed during the heat treatment. EDX point analysis showed that these crystals on top of the surface are mainly composed of Al with a low content of Fe and Cr. From this observation it can be concluded that crack generation took place during quenching from the austenising temperature (1075°C) to room temperature. During the subsequent tempering procedure at 750°C small corrosion products formed on the fresh crack surfaces.

3.2.2. Metallographical examination

The samples look similar in the cross sections concerning the formed layers, the adherence and the structure of the substrate independent of the heat treatment. Cross sectional views of the layer after heat treatment are shown for type A samples (1040°C/0.5 h + 750°C/1h) in Fig. 4(a) and for type B samples (1075°C/0.5

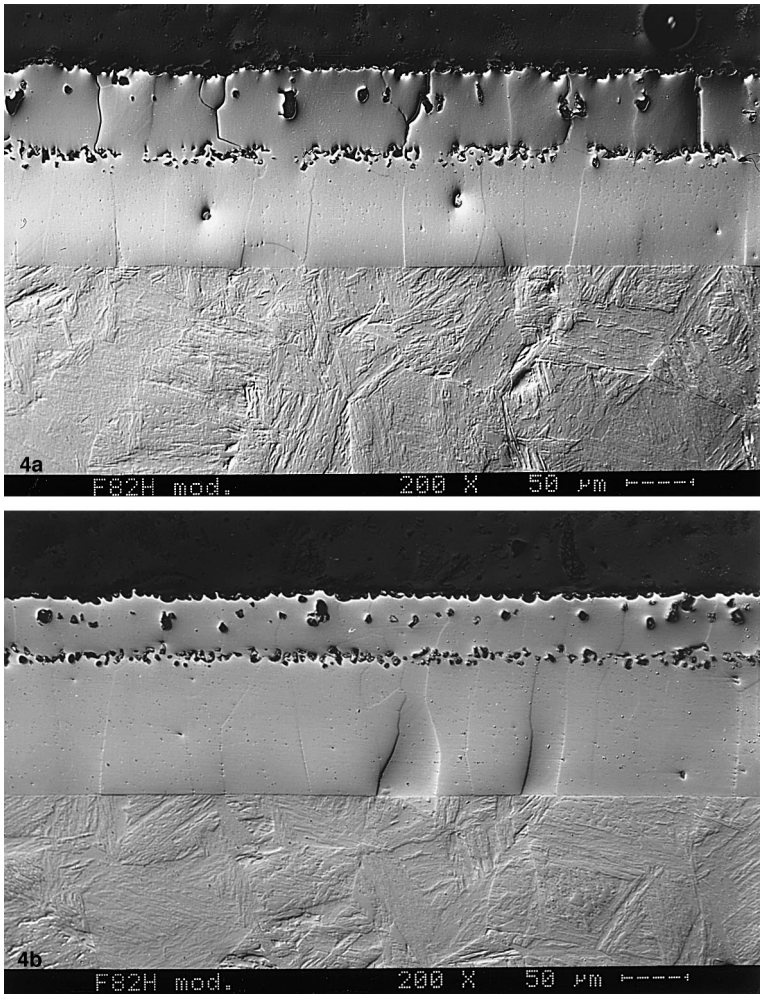

Fig. 4. (a) Cross section of a heat-treated F82H-mod. sample sheet (type A: 1040°C/0.5 h, 750°C/1 h). (b) Cross section of a heat-treated F82H-mod. sample sheet (type B: 1075°C/0.5 h, 750°C/2 h).

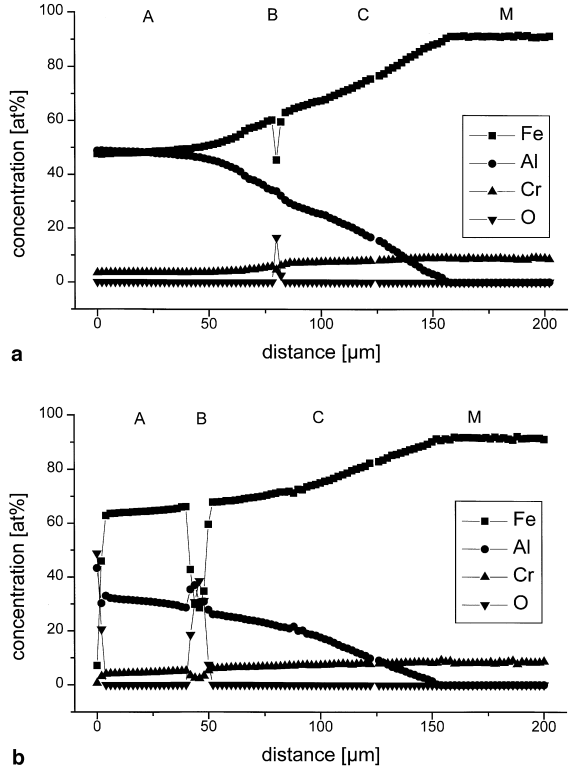

Fig. 5. (a) EPMA line scan of a heat-treated aluminised F82H-mod. sample sheet (type A: 1040°C/0.5 h, 750°C/1 h); A, FeAl; B, band of pores, C, α-Fe(Al), M, matrix. (b) EPMA line scan of a heat-treated aluminised F82H-mod. sample sheet (type B: 1075°C/0.5 h, 750°C/2 h); A, FeAl; B, band of pores; C, α-Fe(Al); M, matrix.

h + 750°C/ 2h) in Fig. 4(b). In the following the results of the metallographical examination will be discussed for types A and B.

In general, the layer can be subdivided into a external layer, an intermediate band of high porosity and an internal layer, which is directly in contact with the substrate. The interface to the substrate beneath the internal layer is indicated as a sharp boundary. The sample surface appears to be rather rough. In the external layer, near the sample surface, a few pores were formed. Additionally, cracks starting from the surface are observed. In most cases they were stopped in the porous zone, in some seldom cases also in the middle of the layer. A crack growth into the internal layer was never recognised. The structure of the layer is characterised by grains oriented perpendicular to the surface. Small needles like precipitations can be observed in the internal layer which are homogeneously distributed. The grain structure beneath the layer has the typical appearance of martensitic substrate.

The thickness of the external layer is dependent on the amount of solidified Al which adheres on the surface after the hot dip aluminising process. On the other hand, the thickness of the internal layer depends on time and temperature used for the heat treatment. Type A samples result in an internal 70 μm is thick layer, type B samples reveal a 90 μm thick layer. Equal values are obtained on MANET sheets treated in the same manner (aluminised and heat treated). This indicates that the diffusion process for the internal layer formation is independent of the ferritic steel used as base material.

3.2.3. Analytical examination

EMPA line scans with a step width of 2 μm were performed on polished cross sections of type A and B samples. The results are shown in Fig. 5(a) and (b). The compositions found for the different layers are identical for both heat treatments A and B. Therefore, the results obtained will be discussed without differentiation between type A and B samples in the following. It can be seen that the intermetallic phase Fe_2Al_5 has completely transformed after the heat treatment. On top there is a high concentration of Al and O on the surface which indicates the formation of an alumina layer (see Fig. 5(b)). Just beneath the surface a stratified FeAl phase is recognised. According to the binary Fe–Al phase diagram [13] (which has been used here rather than the ternary Fe–Cr–Al phase diagram) this phase is stable between 29–54 at.% Al at 1040°C and 30–54.5 at.% at 1075°C, respectively. As already mentioned above, the extension of this zone, the external layer, is dependent on the amount of solidified Al which remained on the surface after the hot-dip aluminising process. The strong scatter of the concentration gradients beneath the FeAl phase results from interactions of the electron beam with pores of the intermediate layer. A correct quantitative analysis is not possible. The Al concentration decreases more rapidly in the internal layer than in the external layer. The Al concentration decreases from 30 to 0 at.% within 70 μm (type A) and 90 μm (type B), respectively. The Fe and Cr contents show the opposite trend. The composition corresponds to the compound α-Fe(Al) according to the binary phase diagram.

Therefore both types of heat treatments, A and B are suitable to transform the brittle Fe_2Al_5 compound into softer, more ductile phases (FeAl and α-Fe(Al)). The same results were obtained for aluminised MANET sheets subsequently heat-treated like type A and B samples [8,9,14].

3.2.4. Vickers microhardness

The observations made for types A and B are the same. Hence, the results obtained for both kinds of samples will be discussed together in the following. The transformation of the brittle Fe_2Al_5 phase into softer,

Table 2
Results of microhardness measurements (HV 0.05) on type A and B samples

	Type A/HV 0.05 1040°C/0.5 h, 750°C/1 h	Type B/HV 0.05 1075°C/0.5 h, 750°C/2 h
External layer FeAl	290–372	225–296
Internal layer α-Fe(Al)	321 (beneath band of pores)	309 (beneath band of pores)
	242	292
	202 (interface coating/steel)	192 (interface coating/steel)
Substrate F82H-mod.	230–250	235–250

more ductile phases can be observed by microhardness measurements. The results are summarised in Table 2.

The microhardness of FeAl (external layer) is constant over the whole area. This is in agreement with EDX measurements which showed a uniform composition of Fe an Al in this region. In the internal layer the Al content changes from around 30 to 0 at.%. This corresponds with the change of the microhardness values in this layer: with decreasing Al content the microhardness decreases as well. The hardness of the substrate remained unchanged compared to the virgin material.

4. Discussion and conclusions

It could be shown, that hot dip aluminising is a suitable method to cover a ferritic steel e.g. F82H-mod. with a homogenous intermetallic layer which adheres well to the steel surface. The 20–30 μm thick Fe_2Al_5 phase has been formed mainly by Al diffusion into the steel substrate. The results of aluminised samples after different heat treatments (type A: 1040°C/0.5 h 750°C/ 1 h and type B: 1075°C/0.5 h, 750°C/2 h) can be summarised as follows:

- The formation of the structure of the coating produced – an internal and external layer separated by a porous band – is independent of the heat applied treatment.
- The heat treatments of types A and B did not influence the composition of the two layers formed. In both cases, the external layer consists of an FeAl phase, the internal one of an α-Fe(Al) phase.
- The thickness of the internal layer is dependent on the heat treatment chosen. In the case of type A (1040°C) this layer is thinner (around 70 μm) than in the case of using type B heat treatment (1075°C) which leads to about 90 μm thick layers. The faster diffusion process at higher temperature is responsible for the increase in thickness of around 20 μm.
- The formation of α-Al_2O_3 was only observed at 1075°C (heat treatment type B) but not at 1040°C (type A). Although α-Al_2O_3 is already thermodynamically stable at this temperature, the heat treatment time was not sufficient to transform the produced alumina into this form.

Further results should be mentioned:

- The layers produced by this manner are compatible with flowing Pb–17Li at 450°C up to 10 000 h [15].
- Self-healing of the alumina layer in the case of cracking or spalling-off should occur as the thermodynamic calculations done under the assumption of an oxygen saturated environment revealed [16,17]. The Al content in the FeAl layer is sufficient.
- The reduction in deuterium permeation rate of up to two orders of magnitude were achieved for aluminised and heat treated samples [18].
- The ITER test module fabrication sequence is not completely clear as yet. Until now, two different ways are under discussion [19] which are both compatible with the coating procedure (hot dip technique and subsequent heat treatment) presented in this paper.

In general, both standard heat treatments, type A (F82H-mod.: 1040°C/0.5 h, 750°C/1 h) and B (MANET: 1075°C/0.5 h, 750°C/2 h), fulfill the goals required for this procedure like complete incorporation of solidified Al, transformation of the brittle Fe_2Al_5 phase into more ductile phases, the formation of a thin alumina layer on the top of the coating, the guarantee of maintaining the original mechanical properties of the steel remains unchanged and the compatibility with the ITM fabrication sequence.

Acknowledgements

The authors wish to thank Mr P. Graf and Mr H. Zimmermann for the metallographic and microhardness examinations and Mr. Deutsch for measuring the XPS spectra. This work has been performed in the framework of the Nuclear Fusion Project of the Forschungszentrum Karlsruhe and is supported by the European communities within the European Fusion Technology program.

References

[1] K.S. Forcey, A. Perujo, F. Reiter, P.L. Lolli-Ceroni, J. Nucl. Mater. 200 (1993) 417.
[2] A. Perujo, K.S. Forcey, T. Sample, J. Nucl. Mater. 207 (1993) 86.

[3] L. Giancarli, L. Baraer, M. Eid, M. Fütterer, E. Proust, X. Raepsaet, J.F. Salavy, L. Sedano, Y. Severi, J. Quintric-Bossy, C. Nardi, L. Petrizzi, Fusion Technol. 26 (1994) 1079.
[4] A. Perujo, E. Serra, H. Kolbe, T. Sample, J. Nucl. Mater. 233–237 (1996) 1102.
[5] H. Glasbrenner, A. Perujo, E. Serra, Fusion Technol. 28 (1995) 1159.
[6] J.D. Fowler, D. Chandra, T.S. Elleman, A.W. Payne, K. Verguse, J. Am. Ceram. Soc. 60 (1977) 155.
[7] H. Glasbrenner, J. Konys, G. Reimann, K. Stein, O. Wedemeyer, Proc. of the 19th Symp. on Fusion Technology, Lisbon Portugal, 1996, 1423.
[8] K. Stein-Fechner, J. Konys, O. Wedemeyer, J. Nucl. Mater. 249 (1997) 33.
[9] K. Stein-Fechner, H. Glasbrenner, J. Konys, O. Wedemeyer, Report FZK 5956, 1997.
[10] T. Sample, P. Fenici, H. Kolbe, L. Orechia, Proc. of the 18th Symp. on Fusion Technology, Karlsruhe, Germany, 1994, p. 1289.
[11] L. Meyer, H.-E. Bühler, Aluminium 43 (1967) 733.
[12] J.C. Fuggle, L.M. Watson, D.J. Fabian, Surf. Sci. 49 (1975) 61.
[13] Th.B. Massalski (Ed.), Binary Alloy Phase Diagrams, 2nd ed., ASM, Metals Park, 1990.
[14] H. Glasbrenner, FZK, unpublished results.
[15] H.U. Borgstedt, H. Glasbrenner, Z. Peric, J. Nucl. Mater. 212–215 (1994) 1501.
[16] P. Hubberstey, T. Sample, A. Terlain, Fusion Technol. 28 (1995) 1194.
[17] H. Kleykamp, H. Glasbrenner, Z. Metallkd. 88 (1997) 230.
[18] E. Serra, H. Glasbrenner, A. Perujo, presented at ISFNT 4, 6.-11.04. 1997, Tokyo, Japan.
[19] M.A. Futterer, L. Giancarli, Report CEA 2090, 1997.